



CHORUS

This is the accepted manuscript made available via CHORUS. The article has been published as:

Electric conductivity of a hot hadron gas from a kinetic approach

Moritz Greif, Carsten Greiner, and Gabriel S. Denicol

Phys. Rev. D **93**, 096012 — Published 26 May 2016

DOI: [10.1103/PhysRevD.93.096012](https://doi.org/10.1103/PhysRevD.93.096012)

Electric Conductivity of a hot hadron gas from a kinetic approach

Moritz Greif* and Carsten Greiner

*Institut für Theoretische Physik, Johann Wolfgang Goethe-Universität,
Max-von-Laue-Str. 1, D-60438 Frankfurt am Main, Germany*

Gabriel S. Denicol

Physics Department, Brookhaven National Lab, Building 510A, Upton, New York 11973, USA

We calculate the electric conductivity of a gas of relativistic particles with isotropic cross sections using the Boltzmann equation as the starting point. Our analysis is restricted to elastic collisions. We show the perfect agreement with previously published numerical results for a massless quark-gluon plasma, and give results for the electric conductivity of an interacting hadron gas, employing realistic resonance cross sections. These results for the electric conductivity of a hot hadron gas, as created in (ultra-)relativistic heavy-ion collisions, are of rich phenomenological as well as theoretical interest and can be compared to, e.g., lattice quantum field theory calculations.

I. INTRODUCTION

In ultrarelativistic heavy ion collisions the core of the fireball can reach temperatures high enough to temporarily produce a new phase of nuclear matter, the quark-gluon plasma (QGP), in which quarks and gluons are the relevant degrees of freedom [1–4]. After a few fm/c (in the center of momentum of the collision), the nuclear matter produced cools down and undergoes a phase transition into a hadronic phase [5]. The hadron gas produced at the late stages of the collision is still hot, with temperatures $\lesssim 160$ MeV, and hadrons can still collide multiple times before they stream freely into the detector.

The theoretical understanding of the experimentally measured data is essential for gaining knowledge of our nature at extreme scales. Among the most successful descriptive pictures of the different phases of nuclear matter are hydrodynamic calculations [6–13], and solutions of the Boltzmann equation (BE) [14–27]. Hydrodynamical calculations describe the QGP [28] and the hadron gas (HG) as a droplet of viscous fluid, and need as an input macroscopic properties of the matter, as the equation of state (EOS) and transport coefficients, like the shear and bulk viscosity. The existence of a finite shear viscosity in the QGP is necessary to explain, e.g., experimental data of the elliptic flow coefficient v_2 [29]. The Boltzmann equation, governing the time development of a particle distribution function due to collisions, allows for a direct computation of transport coefficients, and also the space-time development of the QGP phase can be described numerically [14, 18–20, 23, 24, 26, 27]. In some of these studies, the BE was solved numerically in a fixed box, employing various cross section for a given set of particles. With such a setup, the transport coefficients shear viscosity over entropy density η/s , heat flow κ , as well as the static electric conductivity σ_{el} could be computed directly, see, e.g., Ref. [21, 22, 25, 30–33]. The computation of the latter coefficient in a new, analytic way is the aim of this paper. Using established analytic developments [34–36], we investigated how an equilibrated relativistic gas of electrically charged particles, governed by the BE, behaves upon the influence of a small, static, electric field that is turned on. Assuming that the total system is electrically neutral, naturally an electric current will develop and eventually reach a static value (in an infinitely large system or setting periodic boundary conditions). The longitudinal static electric conductivity σ_{el} relates the response of the electric current¹ \vec{j} to the externally applied static electric field \vec{E} ,

$$\vec{j} = \sigma_{\text{el}} \vec{E}. \quad (1)$$

We can thereby compute σ_{el} for a given set of (massive or massless) particle species in the system and the given set of their mutual, elastic, collision cross section. This is basically an extension to the well-known Drude formula for the electric conductivity (see Sec. III B) for a hadron resonance gas.

The electric conductivity can be related to the diffusion of magnetic fields in a medium [37–39] and the soft dilepton production rate [40–42] of a hot thermal medium. This is a measurable quantity, however, experimental constraints would e.g. require an accurate modelling of heavy-ion collisions, and the theoretical understanding of dilepton yields is still subject of active research [43].

* greif@th.physik.uni-frankfurt.de

¹ More precise, the electrically charged particle diffusion current density

Many scientific groups have recently investigated this transport coefficient, including the mentioned numerical solution of the BE [31, 33], off-shell transport models [44, 45], holography [46], lattice gauge theory [41, 47–55], Dyson-Schwinger calculations [56], analytic calculations within perturbative quantum chromo dynamics (QCD) [57, 58], a dynamical quasiparticle model [59, 60] and chiral perturbation theory [39]. All (but Ref. [46]) of these calculations aim at the value of σ_{el} in the QGP phase, some do extend below the transition temperature towards the HG. In general, the results differ over several orders of magnitude, and comparisons among different approaches are often intriguing. In the HG there has been so far no analytic computation of the electric conductivity from pure kinetic theory, something we will provide in this work. We investigate the influence of masses, average total cross sections, and different species. We finally state the temperature dependent electric conductivity of a hadron gas with well justified approximations. Indeed, the framework can give a very precise answer from kinetic theory for any (charge neutral) elastic particle system, and is not restricted to the results considered in this paper.

This work is organized as follows. In Sec. II we give basic definitions regarding the relativistic formulation for the fluid dynamical quantities. In Sec. III we derive the algorithm for the computation of the conductivity from linear response, and continue in Sec. IV with our results. First, we reproduce previously published numerical results and show the convergence of the method in Sec. IV A, then we show the influence of masses systematically in Sec. IV B, followed by the results for a realistic Pion gas in Sec. IV C, a Pion-Nucleon-Kaon gas with fixed cross sections (Sec. IV D) and realistic cross sections (Sec. IV E). We give a conclusion and outlook in Sec. V.

Our units are $\hbar = c = k = 1$; the space-time metric is given by $g^{\mu\nu} = \text{diag}(1, -1, -1, -1)$. Greek indices run from 0 to 3.

II. BASIC DEFINITIONS

We consider a dilute gas consisting of N_{species} particle species, with the i -th particle species having electric charge q_i and degeneracy g_i . This system is in the presence of an external electromagnetic field, given by an electromagnetic field strength $F^{\mu\nu}$, and its net-electric charge density is assumed to be approximately zero at all space-time points. The state of the system is characterized by the single particle distribution function of each particle species, $f_i(x, p)$. The time evolution equation satisfied by $f_i(x, p)$ is the Boltzmann equation, which is an integro-differential equation with the following general structure

$$k^\mu \frac{\partial}{\partial x^\mu} f_{\mathbf{k}}^i + k_\nu q_i F^{\mu\nu} \frac{\partial}{\partial k^\mu} f_{\mathbf{k}}^i = \sum_{j=1}^{N_{\text{species}}} C_{ij}(x^\mu, k^\mu),$$

where C_{ij} is the collision term, that will be specified later in this work. Since our goal is to calculate the electric conductivity of this system, we shall consider the case of a homogeneous, but time-dependent electric field.

The energy-momentum tensor and net electric charge four-current are expressed as the following momentum integrals of the single-particle distribution function

$$T^{\mu\nu} = \sum_{i=1}^{N_{\text{species}}} \langle k^\mu k^\nu \rangle_i, \quad N_q^\mu = \sum_{i=1}^{N_{\text{species}}} q_i \langle k^\mu \rangle_i$$

where we employ the following notation

$$\langle \dots \rangle_i \equiv g_i \int \frac{d^3 k}{(2\pi)^3 k^0} (\dots) f_{\mathbf{k}}^i.$$

These currents are associated to conserved quantities and satisfy the continuity equations, $\partial_\mu T^{\mu\nu} = 0$ and $\partial_\mu N_q^\mu = 0$.

It is convenient to decompose $T^{\mu\nu}$ and N_q^μ in terms of the fluid's collective velocity field, u^μ . Without loss of generality, these currents are re-expressed as

$$T^{\mu\nu} = \epsilon u^\mu u^\nu - \Delta^{\mu\nu} (P_0 + \Pi) + \pi^{\mu\nu}, \quad (2)$$

$$N_q^\mu(x) = n_q u^\mu + V_q^\mu. \quad (3)$$

Above, we introduced the energy density ϵ , the thermodynamic pressure P_0 , the bulk viscous pressure Π , the shear stress tensor $\pi^{\mu\nu}$, the net electric charge density n_q , and the net electric charge diffusion current V_q^μ . We also defined the spatial projector $\Delta^{\mu\nu} = g^{\mu\nu} - u^\mu u^\nu$ and employed Landau's definition of the fluid velocity as an eigenvector of

$T^{\mu\nu}$ with eigenvalue ϵ , that is, $T^{\mu\nu}u_\nu = \epsilon u^\mu$. In this scheme, each new variable introduced is expressed by a given contraction/projection of the currents with u^μ and $\Delta^{\mu\nu}$,

$$\epsilon = u_\mu u_\nu T^{\mu\nu}, \quad P_0 + \Pi = -\frac{1}{3}\Delta_{\mu\nu}T^{\mu\nu}, \quad (4)$$

$$\pi^{\mu\nu} = \Delta_{\alpha\beta}^{\mu\nu}T^{\alpha\beta}, \quad n_q = u_\mu N_q^\mu, \quad V_q^\mu = N_q^{\langle\mu\rangle}. \quad (5)$$

For convenience, we adopt the notation $A^{\langle\mu\rangle} \equiv \Delta_\nu^\mu A^\nu$ and $A^{\langle\mu\nu\rangle} \equiv \Delta_{\alpha\beta}^{\mu\nu}A^{\alpha\beta}$. The latter definition used the double, traceless, symmetric projection operator $\Delta_{\alpha\beta}^{\mu\nu} = (\Delta_\alpha^\mu \Delta_\beta^\nu + \Delta_\alpha^\nu \Delta_\beta^\mu)/2 - \Delta^{\mu\nu} \Delta_{\alpha\beta}/3$. Since our goal will be to compute the electric conductivity coefficient of a gas, most of the dissipative currents introduced above will play no role in our calculation. Nevertheless, we introduced them above for the sake of completeness.

We can define a temperature and chemical potential for this system using the traditional matching conditions,

$$\epsilon = \epsilon^{\text{eq}}(T, \mu_q), \quad n_q = n_q^{\text{eq}}(T, \mu_q). \quad (6)$$

where ϵ^{eq} and n_q^{eq} are the energy density and net electric charge density of a system in thermodynamic equilibrium with temperature T and chemical potential μ_q . The values of temperature and chemical potential must be inverted from the above equations. With these definitions, we can introduce the local equilibrium distribution function,

$$f_{0,\mathbf{k}}^i = g_i \exp(-u_\mu k^\mu/T + q_i \mu_q/T),$$

and the deviation from equilibrium $\delta f_{\mathbf{k}}^i = f_{\mathbf{k}}^i - f_{0,\mathbf{k}}^i$, where, $\mu_i = q_i \mu_q$ is the chemical potential of the i -th species. Momentum integrals over these distribution functions will be expressed using the following notation

$$\langle \dots \rangle_{i,0} \equiv g_i \int \frac{d^3 k}{(2\pi)^3 k^0} (\dots) f_{0,\mathbf{k}}^i, \quad \langle \dots \rangle_{i,\delta} \equiv g_i \int \frac{d^3 k}{(2\pi)^3 k^0} (\dots) \delta f_{\mathbf{k}}^i.$$

The electric net charge diffusion current then is

$$j^\mu = N_q^{\langle\mu\rangle} = \sum_{i=1}^{N_{\text{species}}} q_i \langle k^\mu \rangle_{i,\delta}.$$

III. LINEAR RESPONSE TO THE ELECTRIC FIELD

The scenario we want to consider here is that of a thermal 'brick' of matter, in which the temperature $T \equiv \beta_0^{-1}$ and chemical potential $\mu_q \equiv \alpha_0^q/\beta_0$ do not vary in space nor time. We generalize the methods proposed in [61–63] to calculate retarded Green's function associated to the response of a multi-component system to an external electric field. We present the general calculation first, using the full linearized collision term, and show afterwards that the formalism reduces to the well-known Drude formula in the relaxation time approximation. In all remaining computations we use the full linearized collision term.

A. General calculation with linearized collision term

We consider a system initially in thermal equilibrium, with $f_{\mathbf{k}}^i = f_{0,\mathbf{k}}^i$ and $F^{\mu\nu} = 0$. We then suddenly turn on a small external electric field. No external magnetic fields are present and we neglect the effect of any induced field. The distribution function acquires an off-equilibrium part, $f_{\mathbf{k}}^i = f_{0,\mathbf{k}}^i + \delta f_{\mathbf{k}}^i$, and the field strength tensor becomes

$$F^{\mu\nu} \rightarrow \delta F^{\mu\nu} = E^\mu u^\nu - E^\nu u^\mu \quad (7)$$

where $E^\mu = u_\nu F^{\mu\nu}$ is the electric field. We write down the linearized BE (similar to [63]), neglecting any term that is second order in δf , $\delta F^{\mu\nu}$, or their product,

$$k^\mu \frac{\partial}{\partial x^\mu} f_{0,\mathbf{k}}^i + k^\mu \frac{\partial}{\partial x^\mu} \delta f_{\mathbf{k}}^i + k_\nu q_i \delta F^{\mu\nu} \frac{\partial}{\partial k^\mu} f_{0,\mathbf{k}}^i = \sum_{j=1}^{N_{\text{species}}} C_{ij}^{(l)}(x^\mu, k^\mu), \quad (8)$$

with $C_{ij}^{(l)}(x^\mu, k^\mu)$ being the linearized collision term. Without loss of generality, we carry out all computations in the local rest frame of the fluid, $u^\mu = (1, 0, 0, 0)$. Since E^μ is orthogonal to the velocity, $u_\mu E^\mu = 0$, we replace $k_\nu E^\nu \rightarrow k_{(\nu)} E^\nu$. Then we have

$$k^\mu \frac{\partial}{\partial x^\mu} \delta f_{\mathbf{k}}^i + \frac{q_i}{T} f_{0,\mathbf{k}}^i k_{(\nu)} E^\nu = \sum_{j=1}^{N_{\text{species}}} C_{ij}^{(l)}(x^\mu, k^\mu). \quad (9)$$

The linearized collision term can be written as an operator \hat{C} acting on δf ,

$$C_{ij}^{(l)}(x^\mu, k^\mu) \equiv \hat{C} \delta f_{\mathbf{k}}^i = \int dK' dP dP' \gamma_{ij} W_{\mathbf{k}\mathbf{k}' \rightarrow \mathbf{p}\mathbf{p}'}^{ij} f_{0,\mathbf{k}}^i f_{0,\mathbf{k}'}^j \left(\frac{\delta f_{\mathbf{p}}^i}{f_{0,\mathbf{p}}^i} + \frac{\delta f_{\mathbf{p}'}^i}{f_{0,\mathbf{p}'}^i} - \frac{\delta f_{\mathbf{k}}^i}{f_{0,\mathbf{k}}^i} - \frac{\delta f_{\mathbf{k}'}^j}{f_{0,\mathbf{k}'}^j} \right) \quad (10)$$

where we use the notation $dK \equiv d^3k / [(2\pi)^3 k^0]$, $\gamma_{ij} = 1 - 1/2\delta_{ij}$ and $W_{\mathbf{k}\mathbf{k}' \rightarrow \mathbf{p}\mathbf{p}'}^{ij} = s\sigma_{ij}(s, \Theta)(2\pi)^6 \delta^{(4)}(k^\mu + k'^\mu - p^\mu - p'^\mu)$. Above, we only considered elastic 2-to-2 collisions. The total cross section $\sigma_{\text{tot},ij}(s)$ is related to the differential cross section $\sigma_{ij}(s, \Theta)$ in the following way,

$$\sigma_{\text{tot},ij}(s) = \frac{2\pi}{\nu} \int d\Theta \sin \Theta \sigma_{ij}(s, \Theta), \quad \cos \Theta = \frac{(k - k')(p - p')}{(k - k')^2}, \quad s = (k + k')^2. \quad (11)$$

We take the Fourier transform of the Eq. (9), and divide it by the energy $E_{\mathbf{k}} = \sqrt{\mathbf{k}^2 + m^2}$, leading to the following equation for the Fourier transform of the nonequilibrium distribution function, $\delta \tilde{f}_{\mathbf{k}}^i$,

$$\begin{aligned} -i\omega \delta \tilde{f}_{\mathbf{k}}^i + i \frac{\mathbf{k}}{E_{\mathbf{k}}} \cdot \mathbf{q} \delta \tilde{f}_{\mathbf{k}}^i - \sum_{j=1}^{N_{\text{species}}} \frac{1}{E_{\mathbf{k}}} \hat{C}_{ij} \delta \tilde{f}_{\mathbf{k}}^i &= -\frac{q_i}{T E_{\mathbf{k}}} f_{0,\mathbf{k}}^i k_{(\nu)} \tilde{E}_\nu \\ \Rightarrow \delta \tilde{f}_{\mathbf{k}}^i &= -\frac{1}{T} \frac{q_i}{-i\omega + i \frac{\mathbf{k}}{E_{\mathbf{k}}} \cdot \mathbf{q} - \sum_{j=1}^{N_{\text{species}}} \frac{1}{E_{\mathbf{k}}} \hat{C}_{ij}} f_{0,\mathbf{k}}^i \frac{k_{(\nu)}}{E_{\mathbf{k}}} \tilde{E}_\nu, \end{aligned} \quad (12)$$

where \tilde{E}_ν is the Fourier transform of E_ν and the last equation is the formal solution for the distribution function in Fourier space. Using the formal solution derived for $\delta \tilde{f}_{\mathbf{k}}^i$ in Eq. (12), we can express the Fourier transform of the net electric charge current in the following simple form

$$\tilde{j}^\mu = - \sum_{i=1}^{N_{\text{species}}} \frac{q_i}{T} \int dK k^{(\mu)} \frac{q_i}{-i\omega + i \frac{\mathbf{k}}{E_{\mathbf{k}}} \cdot \mathbf{q} - \sum_{j=1}^{N_{\text{species}}} \frac{1}{E_{\mathbf{k}}} \hat{C}_{ij}} f_{0,\mathbf{k}}^i \frac{k_{(\nu)}}{E_{\mathbf{k}}} \tilde{E}_\nu \equiv \tilde{G}_R^{\mu\nu}(\omega, \mathbf{q}) \tilde{E}_\nu, \quad (13)$$

where we introduced the retarded Green's Function $\tilde{G}_R^{\mu\nu}(\omega, \mathbf{q})$.

In order to compute the static electric conductivity, it will be enough to compute the retarded Greens function $\tilde{G}_R^{\mu\nu}(\omega, \mathbf{q})$ at vanishing frequency and wavenumber, $\tilde{G}_R^{\mu\nu}(0, \mathbf{0})$. For this purpose, we introduce a vector $B_i^\alpha(Q, K_i)$, which satisfies the following integro-differential equation

$$\left[-i\omega + i \frac{\mathbf{k}}{E_{\mathbf{k}}} \cdot \mathbf{q} - \sum_{j=1}^{N_{\text{species}}} \frac{1}{E_{\mathbf{k}}} \hat{C}_{ij} \right] B_i^\alpha(Q, K_i) = q_i f_{0,\mathbf{k}}^i \frac{k^{(\alpha)}}{E_{\mathbf{k}}}. \quad (14)$$

Once B^α is known, the solution for $\tilde{G}_R^{\mu\nu}(\omega, \mathbf{q})$ follows trivially as

$$\tilde{G}_R^{\mu\nu}(\omega, \mathbf{q}) = - \sum_{i=1}^{N_{\text{species}}} \frac{q_i}{T} \int dK k^{(\mu)} B_i^{(\nu)}(Q, K_i). \quad (15)$$

Strictly speaking, B^α is a general function of $Q = (\omega, \mathbf{k})$, however, since we will need it only at vanishing Q , it is sufficient to only consider its dependence on the 4-momentum K , that is, $B_i^\alpha(Q = 0, K_i)$. We know that $B_i^\alpha(K)$ is a 4-vector orthogonal to u^μ and its tensor structure must be constructed from combinations of u^μ , k^μ , and $g^{\mu\nu}$. Therefore, it must be a tensor of the following form, $B_i^\alpha(K) \sim k^{(\alpha)}$, with the proportionality factors being functions of the scalars μ_q , T , and $E_{\mathbf{k}}$. It is convenient to express it as an expansion in powers of the energy,

$$B_i^\alpha(K) = f_{0,\mathbf{k}}^i k^{(\alpha)} \sum_{n=0}^{\infty} a_n^{(i)} E_{\mathbf{k}}^n, \quad (16)$$

where $a_n^{(i)}$ are the expansion coefficients. Using the well-known relation

$$\int dK k^{(\mu)} k^{(\nu)} E_{i,\mathbf{k}}^n f_{0,\mathbf{k}}^i = \frac{1}{3} \Delta^{\mu\nu} \int dK E_{\mathbf{k}}^n f_{0,\mathbf{k}}^i \Delta_{\alpha\beta} k^\alpha k^\beta, \quad (17)$$

together with Eqs. (15) and (16), it is possible to express the retarded Green's function in terms of the coefficients $a_n^{(i)}$,

$$\tilde{G}_R^{\mu\nu}(0, \mathbf{0}) = -\Delta^{\mu\nu} \sum_{i=1}^{N_{\text{species}}} \sum_{n=0}^{\infty} \frac{q_i}{3T} a_n^{(i)} \int dK f_{0,\mathbf{k}}^i E_{\mathbf{k}}^n \Delta_{\alpha\beta} k^\alpha k^\beta \equiv \Delta^{\mu\nu} \tilde{G}_R. \quad (18)$$

Above, we defined the scalar retarded Green's function

$$\tilde{G}_R = - \sum_{i=1}^{N_{\text{species}}} \sum_{n=0}^{\infty} \frac{q_i}{3T} a_n^{(i)} \int dK E_{\mathbf{k}}^n (\Delta_{\mu\nu} k^\mu k^\nu) f_{0,\mathbf{k}}^i,$$

which can be used to express the linear relation between current and driving electric field at $Q = 0$ as

$$\tilde{j}^\mu = \tilde{G}_R \tilde{E}^\mu.$$

The above relation allows us to identify the electric conductivity as $\sigma_{\text{el}} \equiv \tilde{G}_R$.

Naturally, the expansion (16) must be truncated at some point and we will discuss the convergence of our results to the order of the truncation. We note that, even at the lowest possible order of truncation, the resulting transport coefficients are expected to be accurate up to 10 %, see, e.g., [34, 64]. Our next step is the determination of the expansion coefficients $a_n^{(i)}$. Multiplying Eq. (14) with $E_{\mathbf{k}}^m k^{(\beta)}$ and integrating over momentum we get an equation for $a_n^{(i)}$,

$$\sum_{n=0}^{\infty} \int dK_i E_{\mathbf{k}}^{m-1} k^{(\beta)} \left[- \sum_{j=1}^{N_{\text{species}}} \hat{C}_{ij} f_{0,\mathbf{k}}^i E_{\mathbf{k}}^n k^{(\alpha)} a_n^{(i)} \right] = q_i \int dK_i E_{\mathbf{k}}^{m-1} k^{(\alpha)} k^{(\beta)} f_{0,\mathbf{k}}^i.$$

Using straightforward manipulations of this equation and the above definition of the collision term, Eq. (10), we can rewrite it in the following form,

$$\sum_{n=0}^{\infty} \sum_{j=1}^{N_{\text{species}}} [\mathcal{A}_{mn}^i \delta^{ij} + \mathcal{C}_{mn}^{ij}] a_n^{(j)} = b_m^i,$$

where we defined

$$\begin{aligned} \mathcal{A}_{mn}^i &= \sum_{j=1}^{N_{\text{species}}} \int dK_i dK'_j dP_i dP'_j \gamma_{ij} W_{\mathbf{k}\mathbf{k}' \rightarrow \mathbf{p}\mathbf{p}'}^{ij} f_{0,\mathbf{k}}^i f_{0,\mathbf{k}'}^j E_{i,\mathbf{k}}^{m-1} k_{(\alpha)} \left(E_{i,\mathbf{p}}^n p^{(\alpha)} - E_{i,\mathbf{k}}^n k^{(\alpha)} \right), \\ \mathcal{C}_{mn}^{ij} &= \int dK_i dK'_j dP_i dP'_j \gamma_{ij} W_{\mathbf{k}\mathbf{k}' \rightarrow \mathbf{p}\mathbf{p}'}^{ij} f_{0,\mathbf{k}}^i f_{0,\mathbf{k}'}^j E_{i,\mathbf{k}}^{m-1} k_{(\alpha)} \left(E_{j,\mathbf{p}}^n p'^{(\alpha)} - E_{i,\mathbf{k}'}^n k'^{(\alpha)} \right), \\ b_m^i &= q_i \int dK E_{\mathbf{k}}^{m-1} (-\Delta^{\mu\nu} k_\mu k_\nu) f_{0,\mathbf{k}}^i. \end{aligned} \quad (19)$$

For later use we denote the above matrix in particle species space and expansion space as

$$\mathcal{N}_{mn}^{ij} \equiv \mathcal{A}_{mn}^i \delta^{ij} + \mathcal{C}_{mn}^{ij}. \quad (20)$$

Note that there is no sum over i implied. The Landau matching condition can also be expressed as

$$\Delta_\nu^\lambda u_\mu T^{\mu\nu} = \sum_{i=1}^{N_{\text{species}}} \int dK u_\nu k^\nu k^{(\mu)} \delta f_{\mathbf{k}}^i = -\frac{1}{3T} \sum_{i=1}^{N_{\text{species}}} \sum_{n=0}^{\infty} a_n^{(i)} \int dK f_{0,\mathbf{k}}^i E_{\mathbf{k}}^{n+1} (\Delta^{\alpha\beta} k_\alpha k_\beta) \tilde{E}^\mu = 0.$$

Since this should be true for any electric field and any of its components, we obtain a constraint that must be satisfied by the coefficients $a_n^{(i)}$,

$$\begin{aligned} \sum_{i=1}^{N_{\text{species}}} \sum_{n=0}^{\infty} a_n^{(i)} \left[\int dK f_{0,\mathbf{k}}^i E_{\mathbf{k}}^{n+1} (\Delta^{\alpha\beta} k_{\alpha} k_{\beta}) \right] &= 0 \\ \Rightarrow \sum_{i=1}^{N_{\text{species}}} \sum_{n=0}^{\infty} a_n^{(i)} d_n^i &= 0 \quad \text{with} \quad d_n^i \equiv \int dK f_{0,\mathbf{k}}^i E_{\mathbf{k}}^{n+1} (\Delta^{\alpha\beta} k_{\alpha} k_{\beta}). \end{aligned} \quad (21)$$

Solving the integrals in Eq. (19) for a given set of species and cross sections allows us to obtain the unknown coefficients $a_n^{(i)}$ by inverting the matrix $\mathcal{A}_{mn}^i \delta^{ij} + \mathcal{C}_{mn}^{ij}$ along with condition (21). In practice, this amounts to removing one line and column from the matrix \mathcal{N}_{mn}^{ij} .

B. Relaxation time limit

Nonrelativistically, the Drude formula for the electric conductivity $\sigma_{\text{el,nr}}$ of a single charge carrying species (e.g. electrons) with charge q_e , density n_e and mass m_e reads

$$\sigma_{\text{el,nr}} = \frac{n_e q_e^2 \tau}{m_e}, \quad (22)$$

where τ is the mean time between collisions of the charge carriers (e.g. electrons) with, e.g., atomic cores. The Boltzmann equation can be solved analytically in the relaxation time approximation, which corresponds to a simplistic model for the collision term,

$$p^{\mu} \partial_{\mu} f_q + q F^{\alpha\beta} p_{\beta} \frac{\partial f_q}{\partial p^{\alpha}} = -\frac{p^{\mu} u_{\mu}}{\tau} (f_q - f_{\text{eq},q}). \quad (23)$$

It allows for a straightforward calculation of the charged particle distribution f_q after applying an external electric field. The uncharged particle distribution remains thermal $f_{q=0} = f_{\text{eq},q=0}$ and is not affected by the electric field,

$$\sigma_{\text{el}} = \frac{1}{3T} \sum_{i=1}^{N_{\text{species}}} q_i^2 n_i \tau. \quad (24)$$

Here, τ is the mean time between collisions of particles, independent of the particle type; for more details, see, e.g., Ref. [31]. Using Eq. (15) with a relaxation time collision operator we recover the relaxation time answer, Eq. (24), for the electric conductivity,

$$\begin{aligned} \tilde{j}^{\mu} &= \sum_{i=1}^{N_{\text{species}}} \frac{(q_i)^2}{T} \int dK k^{(\mu)} \frac{1}{-\sum_{j=1}^{N_{\text{species}}} \hat{C}_{ij}} f_{0,\mathbf{k}}^i k^{(\nu)} \tilde{E}_{\nu} \\ &= \sum_{i=1}^{N_{\text{species}}} \frac{(q_i)^2}{T} \int dK k^{(\mu)} \frac{\tau}{E_{\mathbf{k}}} f_{0,\mathbf{k}}^i k^{(\nu)} \tilde{E}_{\nu} \\ &= \sum_{i=1}^{N_{\text{species}}} \frac{(q_i)^2 \tau}{3T} \left[\int dK \frac{1}{E_{\mathbf{k}}} (\Delta^{\alpha\beta} k_{\alpha} k_{\beta}) f_{0,\mathbf{k}}^i \right] \tilde{E}^{\mu} \\ &= \sum_{i=1}^{N_{\text{species}}} \frac{(q_i)^2 \tau}{3T} n_{0,i} \tilde{E}^{\mu}. \end{aligned} \quad (25)$$

IV. RESULTS

Our main goal is to calculate the electric conductivity of a hadron gas characterized by (measured) hadron-hadron cross sections (e.g. Breit-Wigner peaked resonances). In practice we have to limit the calculation to the dominant

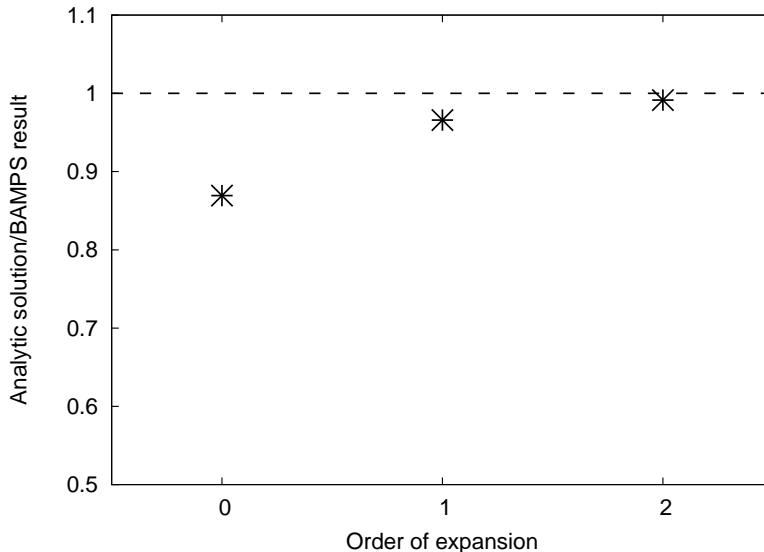


Figure 1. Convergence of the analytical computation for the electric conductivity for a massless quark-gluon gas towards the numerical value obtained by the partonic cascade BAMPS ([31])

hadron species, such as pions, protons, neutrons, kaons. To understand the results and to cross check our method, we work systematically and include more species, masses and cross sections step-by-step. The use of simplified hadronic cross sections is common practise, e.g. in Ref. [65] the authors model a multicomponent hadron gas with species dependent constant cross sections in order to compute shear viscous phase space corrections. The authors of Ref. [63] compute the hadronic shear viscosity over entropy ratio using different constant cross sections for meson-meson, meson-baryon and baryon-baryon scattering.

A. Massless particles and constant isotropic cross sections

As a first step, we compute the electric conductivity for a massless gas of charged and uncharged particles, colliding with a fixed value of the cross section σ_{tot} , which is assumed to be constant. We give the result for the matrix in Eq. (20), which we truncate at $n = 2$. We define $\bar{n}_{ij} = (\delta_{ij}n_i n_T - n_i n_j)$, with $n_T = \sum_i^{N_{\text{species}}} n_i$ being the total particle density. The matrix is

$$\mathcal{N}_{mn}^{ij} = \begin{pmatrix} \mathcal{N}_{00}^{ij} & \mathcal{N}_{10}^{ij} & \mathcal{N}_{12}^{ij} \\ \mathcal{N}_{10}^{ij} & \mathcal{N}_{11}^{ij} & \mathcal{N}_{12}^{ij} \\ \mathcal{N}_{20}^{ij} & \mathcal{N}_{21}^{ij} & \mathcal{N}_{22}^{ij} \end{pmatrix} = \sigma_{\text{tot}} \begin{pmatrix} \frac{15}{2} T^2 \bar{n}_{ij} & 36 T^3 \bar{n}_{ij} & 210 T^4 \bar{n}_{ij} \\ 36 T^3 \bar{n}_{ij} & T^4 (216 \delta_{ij} n_i n_T - 192 n_i n_j) & T^5 (1520 \delta_{ij} n_i n_T - 1240 n_i n_j) \\ 210 T^4 \bar{n}_{ij} & T^5 (1520 \delta_{ij} n_i n_T - 1240 n_i n_j) & T^6 (12510 \delta_{ij} n_i n_T - 8850 n_i n_j) \end{pmatrix}.$$

This is the key information to obtain the electric conductivity at order 0 + 1 + 2 in the above energy expansion for arbitrary many massless particle species. In order to compare with previously published numerical solutions of the BE, we give the explicit result for a gas of seven species, with electric charges (in units of e) $q_{1,3} = 1/3, q_{2,4} = -1/3, q_5 = 2/3, q_6 = -2/3, q_7 = 0$ and degeneracies $g_{1,2,3,4,5,6} = 6, g_7 = 16$, which mimic a quark-gluon plasma. Using that $e^2 = 4\pi/137$, and considering a cross section of $\sigma_{\text{tot}} = 3$ mb, we obtain the following value of conductivity for this system,

$$\sigma_{\text{el}} = \frac{0.000832737 \text{ GeV}^2}{T}. \quad (26)$$

In Ref. [31] the ultrarelativistic BE was solved for exactly this configuration (using the partonic cascade BAMPS), and the result matches the analytic computation of this paper, Eq. (26), by about 99%. By changing the order of the expansion, we show in Fig. 1, that the result converges for the considered order in expansion (truncation of the sum in Eq. (16) at $n = 2$).

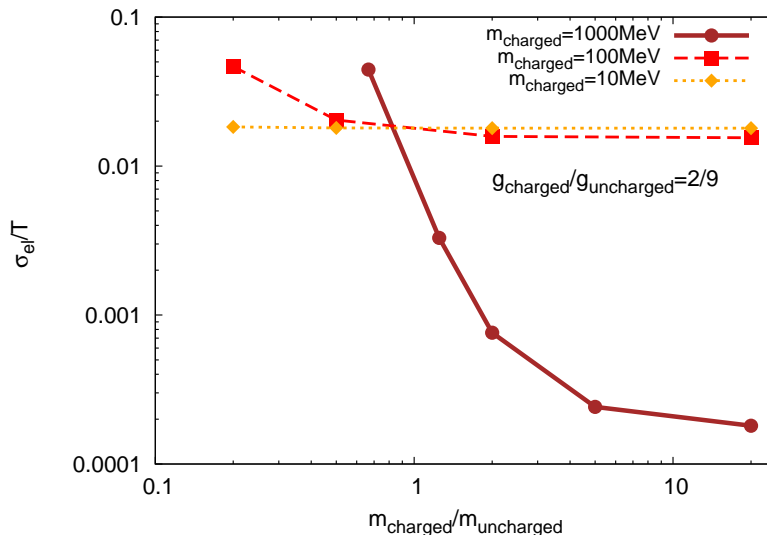


Figure 2. The mass dependence of the electric conductivity for (three species of) interacting relativistic particles. The cross section was arbitrarily fixed to 10 mb, and the degeneracy ratio of charged/uncharged species is 2/9, the charges are $\pm 1, 0$. On the x-axis we vary the mass ratio of the charged to the uncharged species, and show results for different masses of the charged species. (color online)

B. Influence of masses to the electric conductivity

In order to see the influence of sizeable masses to the electric conductivity, we consider an arbitrary, simplified scenario for illustrative purposes. There are three species present, one species with charge +1, degeneracy 1, one with charge -1, degeneracy 1, and one with zero charge and degeneracy 9. All particles have masses, and we vary the ratio of the mass of the charged species with respect to the mass of the uncharged species. In Fig. 2 we show the results for the electric conductivity over temperature depending on this ratio, for different absolute values of the mass of the charged species. There we fix the cross section to an arbitrary value (10 mb) and set the temperature to be 140 MeV and the chemical potential is $\mu_q = 0$. This is a useful exercise to illustrate the mass dependence. In thermal and chemical equilibrium, lower mass particles are more abundant than higher mass particles, and one sees clearly the dependence of the electric conductivity to the number-density ratio of charged to uncharged particles. The electric conductivity is clearly very dependent on both the mass (or density) ratio of charged/uncharged species, and also on the mass (or density) of the charge carrying species. However, the precise values need to be computed (finally via numerical integration) as explained in Sec. III.

C. Pion Gas

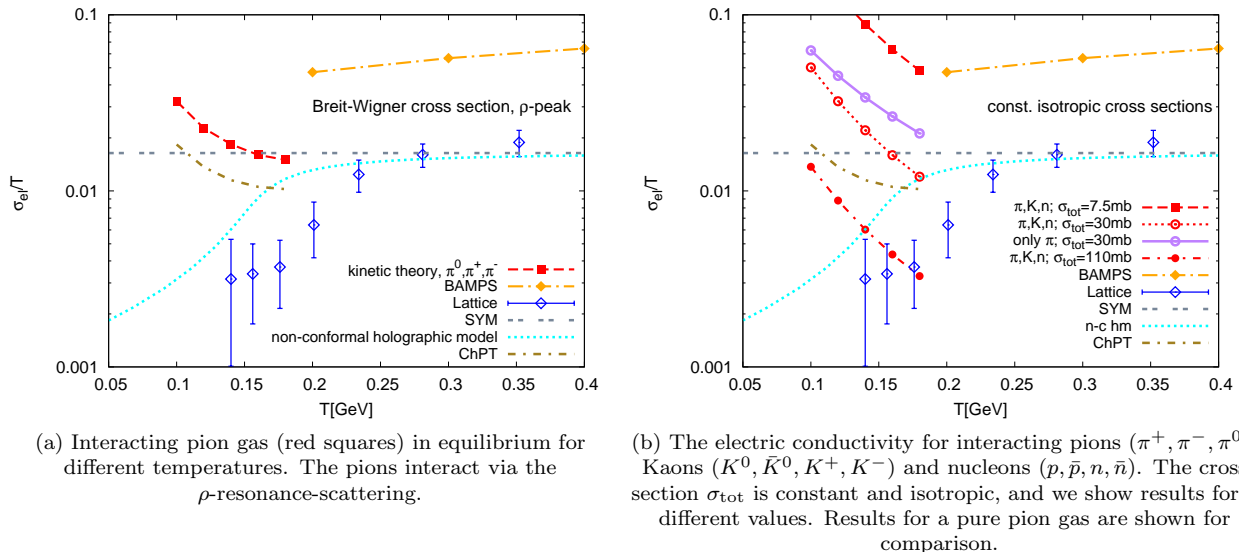
Pions are the most abundant hadrons in an equilibrated hadron gas. Therefore a pure pion gas can be considered a good starting point to understand some features of a realistic hadron gas. We set the chemical potential to zero for simplicity. Mainly, pions interact via the formation and decay of a ρ -resonance (see App. B). In Fig. 3(a) we give results for 3 pion species π^+, π^-, π^0 , interacting via Mandelstam s-dependent (isotropic) resonance cross sections, where we include the dominant ρ -meson peak. Clearly, the electric conductivity approaches a minimum below ~ 180 MeV. This can be physically motivated, as transport coefficients like the conductivity are expected to show a minimum in the QGP-hadron crossover region. This region is now believed to be in the vicinity of ~ 154 MeV [66].

In Fig. 3(a) we compare our results with the results from different groups. The brown dash-dotted line represents calculations using Chiral Perturbation Theory (ChPT) [39] and include only pions. The ChPT-based analysis uses the Green-Kubo formula to extract the conductivity from the spectral function, identifying the dominant diagrams in a low energy and low temperature expansion and implementing unitarity of the partial waves in the thermal width. The temperature dependence of the results from ChPT is very similar to those found in our results, although the overall magnitude of our electric conductivity is about a factor of ~ 1.6 higher. The blue open diamonds are results obtained from lattice QCD calculation for an 2+1d anisotropic and unquenched lattice, Ref. [47]. However, the authors discuss that the lattice data especially around the phase transition should be treated with caution (see Ref. [47] for details).

The grey dashed line is the result obtained in a conformal Super-Yang Mills plasma [67]. In Ref. [46, 68], the authors used a non-conformal, bottom up holographic model to compute the electric conductivity (cyan dotted line). The full orange diamonds are results from the pQCD-based partonic cascade BAMPS [31], employing a running coupling, leading order, Debye-screened pQCD interactions including elastic and inelastic (radiative) scattering of gluons, up, down and strange quarks.

D. Pion-Kaon-Nucleon Gas with constant cross sections

Constant isotropic cross sections are often used to compare different models or theories. In Fig. 3(b) we show results for the electric conductivity for a gas of pions (π^+ , π^- , π^0 ; $m = 138$ MeV), Kaons (K^0 , \bar{K}^0 , K^+ , K^- ; $m = 496$ MeV) and nucleons (p , \bar{p} , n , \bar{n} ; $m = 938$ MeV), all interacting with a constant cross section σ_{tot} . The chemical potential is again zero. We tune this cross section, in order to meet other calculations at the transition temperature from hadrons to the QGP. Strongly coupled theories and 2+1d non-quenched lattice require cross section values of 30 – 110 mb, whereas the pQCD-based partonic cascade BAMPS needs a value of ~ 7.5 mb. These numbers should be taken with care, as we are dealing here with an oversimplified scenario of effective average cross sections. Especially as one approaches the crossover region, this concept is questionable, however it allows to gain some understanding about the effective coupling strength of different theories. In Fig.3(b), the full purple line includes only pions, and uses $\sigma_{\text{tot}} = 30$ mb. By comparing with the dashed red line (all species), one sees the influence of other, heavier species. Also the temperature dependence changes slightly. This is due to the fact, that the ratio of densities of different species is temperature dependent, as the mass enters here as an additional scale. Different contributing massive species can thus result in different temperature behaviour of the conductivity. We expect, that the inclusion of even more species, albeit not very abundant, may decrease the electric conductivity. This may be true even in the case of realistic s -dependent cross sections, cf. Sec. IV E.



(a) Interacting pion gas (red squares) in equilibrium for different temperatures. The pions interact via the ρ -resonance-scattering.

(b) The electric conductivity for interacting pions (π^+ , π^- , π^0), Kaons (K^0 , \bar{K}^0 , K^+ , K^-) and nucleons (p , \bar{p} , n , \bar{n}). The cross section σ_{tot} is constant and isotropic, and we show results for 4 different values. Results for a pure pion gas are shown for comparison.

Figure 3. Results for the electric conductivity from this work and other theories. Parton transport BAMPS [31], Chiral Perturbation Theory ChPT [39], SYM theory [67], a non-conformal holographic model (n-c hm) [46] and lattice [47, 50] calculations are shown for comparison. These theories all require very different effective cross sections when compared to kinetic theory. (color online)

E. Pion-Kaon-Nucleon Gas with experimental cross sections

The calculation procedure presented in this paper becomes gradually more complicated as more particle species are included, with the final numerical integrations becoming rather tedious and time consuming. Furthermore, all cross sections among all species have to be known, something quite problematic in the hadronic zoo. In order to get a rough picture of the electric conductivity in a hadron gas, we use pions, kaons and nucleons as in the previous section, but include now as realistic cross sections as possible, as shown in Tab.I. Many of them are approximated by constant

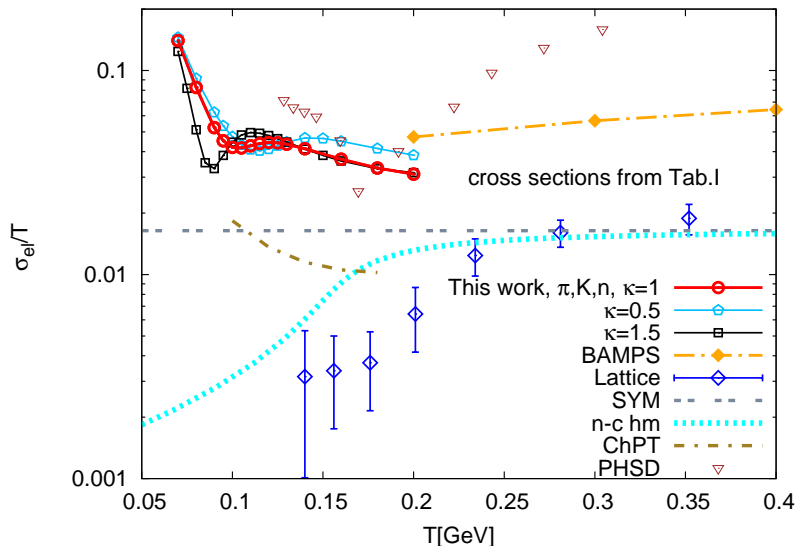


Figure 4. Results for the electric conductivity from this work, including pions, kaons and nucleons, compared to results from PHSD [44, 45] and all other theories as before. All constant cross sections (see Tab. I) are multiplied with a factor κ , which we change in the range of $\kappa = 0.5, 1, 1.5$ in order to get a feeling for the uncertainty. (color online)

values, but we include different resonances. The chemical potential is zero. The result is shown in Fig. 4. In order to get a handle on the uncertainty introduced by using approximated constant cross sections $\sigma_{\text{const.}}$ we multiply these with a factor κ , $\sigma_{\text{const.}} \rightarrow \sigma_{\text{const.}} \kappa$, and vary $\kappa = 0.5, 1, 1.5$. The change of the conductivity is visible but not dramatic. Due to the presence of charged kaons (and nucleons, these are not as important), the conductivity is now higher (30 – 130%) compared to the pure pion case from Fig. 3(a). The dip in the conductivity at around $T = 100$ MeV is prominent. To explain this feature, we note first that the mean invariant collision energy $\langle\sqrt{s}\rangle$ from the $2 \leftrightarrow 2$ collisions, whose effect we are effectively studying, is temperature dependent. For some combinations of species and temperatures, $\langle\sqrt{s}\rangle$ lies in the region of a resonance peak, thus the electric conductivity decreases. However, one has to be cautious, as this dip in the conductivity will disappear or shift for another choice of the set of cross sections, or the inclusion of more resonances. This can be seen by the fact, that the dip moves as we vary κ . The temperature dependence of σ_{el}/T at low T is roughly $\sim T^{-2} - T^{-6}$ depending on the cross sections. This is due to the overall $\sim T^{-2}$ behaviour just by definition (cf. Eq. (24)) combined with the nontrivial ratio of densities (where the masses enter as additional scale) weighted by electric charge and cross sections². As can be seen by comparing with Fig. 3(b), the overall magnitude in our case is dominated by the constant cross section values, mostly ~ 10 mb in the important channels. Although results have to be taken with care due to the uncertainties in the cross sections, they are (to our knowledge) the first (semi-)analytic kinetic computation of the electric conductivity in the hadronic sector for multiple species.

In Fig. 4 we also compare to results from the Parton-Hadron-String Dynamics (PHSD) approach [44, 45]. PHSD is in the hadronic sector a covariant extension to the Boltzmann-Uehling-Uhlenbeck model [69]. The authors apply an electric current to the numerical simulation in thermal equilibrium and observe a static current in order to extract the electric conductivity. The hadronic sector contains several mesons and baryons with resonance cross sections. Their results (triangles) are in the same order of magnitude as ours, and closer than the results from other groups.

V. CONCLUSIONS

In summary, we have developed an analytic formalism to compute the electric conductivity of relativistic, massless or massive gases, governed by the linearized Boltzmann equation including elastic scattering. We use the full linearized collision term, and are able to include arbitrary cross section parametrizations. Naturally, all species in a thermal medium can interact with each other and charged species contribute to the electric current, whereas uncharged species

² The temperature dependence of the resonance cross sections enters through the temperature dependence of the average Mandelstam- s .

	π^+	π^-	π^0	K^+	K^-	K^0	\bar{K}^0	p	n	\bar{p}	\bar{n}
π^+	10	ρ	ρ	10	10	K^*	10	Δ	10	10	Δ
π^-		10	ρ	K^*	10	10	K^*	10	Δ	Δ	10
π^0			5	K^*	10	K^*	K^*	Δ	Δ	Δ	Δ
K^+				10	10	10	50	6	10	20	10
K^-					10	50	10	20	10	6	10
K^0						10	50	6	6	20	20
\bar{K}^0							10	8	20	6	6
p								20	20	100	20
n									20	20	100
\bar{p}										10	10
\bar{n}											10

Table I. The cross sections we used among all species. Numbers are in mb, ρ, K^* and Δ denote Breit-Wigner shaped cross sections with those resonances. Values taken from [70–73]. Complicated or unknown functional forms are approximated by an average constant value. The results depend modestly on the choice of these parametrisations, compare also the results from Sec.IV D)

act as a resistance for the current. The formalism can be reduced to the well-known Drude formula for the electric conductivity. It involves a complicated matrix inversion, and, to be exact, the computation of infinitely many kinetic integrals. For massive species, these have to be evaluated using numerical integration methods. The expansion we make converges rather fast. By comparing to previously published numerical results for the massless case we find excellent agreement. The formalism is quite general and can be extended in various ways, thus we start by investigating the dependence of the conductivity to masses and mass ratios of charged to uncharged species. Ultimately, we use the formalism to present results for the electric conductivity of a massive pion gas, including all pion species, and experimentally measured (Breit-Wigner resonance) cross-sections. We see in accordance with other published results, that the conductivity decreases with increasing temperature, approaching results from a non-conformal holographic model. The temperature dependence is very similar to results from ChPT. Furthermore we include pions, kaons and nucleons with their masses, and present results for a constant isotropic cross section. In this simplified case we can obtain effective cross sections in the range from $\sim 7 - 100$ mb when compared to other theories as pQCD parton transport or lattice. We extend the study further, and present results using a set of approximated realistic cross sections, including resonances. In the present paper, we restrict the results to zero chemical potential. The influence of chemical potentials will be addressed in future. Clearly, the limiting factor is the lack of precise knowledge of elastic cross sections among the hadrons, and our results depend on the choice of their parametrisation. Unknown or complicated cross sections can only be approximated by energy independent constants. However, we believe that the inclusion of fairly realistic cross sections involving pions and kaons, including the ρ, Δ and K^* resonance renders the result physical. The cross sections among protons or neutrons play only a minor role for the final result, as these particles are less abundant due to their mass³. The approximation we made by neglecting heavier particles is thus well justified, however, in future, the study can naturally be extended to include more particle species and their resonances. It is also possible to compute other transport coefficients in a similar fashion.

VI. ACKNOWLEDGMENTS

MG is grateful to “Helmholtz Graduate School for Heavy Ion research”. GSD is supported under DOE Contract No. DE- SC0012704. The authors are grateful to the Center for Scientific Computing (CSC) Frankfurt for the computing resources. This work was supported by the Helmholtz International Center for FAIR within the framework of the LOEWE program launched by the State of Hesse.

³ As a note, only processes involving electrically charged particles contribute, e.g. the neutron-neutron cross section is actually irrelevant.

Appendix A: Calculations of the collision integrals

In the calculations of the matrix elements, the following integrals have to be solved. We will show only some examples, all other integrals can be worked out in a similar fashion. Consider the following integral,

$$\int dP dP' (2\pi)^6 s \sigma_{ij}(s, \Theta) \delta^{(4)}(k^\mu + k'^\mu - p^\mu - p'^\mu) p^\alpha \equiv \Gamma^\alpha. \quad (\text{A1})$$

We define a unitless vector (normalized total momentum of the collision) $\tilde{P}_T^\mu = (k^\mu + k'^\mu)/\sqrt{s}$, and the projection orthogonal to it, $\Delta_P^{\mu\nu} = g^{\mu\nu} - \tilde{P}_T^\mu \tilde{P}_T^\nu$. The tensor Γ^α can only depend on \tilde{P}_T^α , so we can decompose,

$$\Gamma^\alpha = a(s) \tilde{P}_T^\alpha, \quad a(s) = \tilde{P}_T^\alpha \Gamma_\alpha \quad (\text{A2})$$

where

$$a_{ij}(s) = \gamma_{ij} \int dP dP' (2\pi)^6 s \sigma_{ij}(s, \Theta) \delta^{(4)}(k_i^\mu + k_j'^\mu - p_i^\mu - p_j'^\mu) (p_i^\alpha \tilde{P}_{T,\alpha}). \quad (\text{A3})$$

We can always evaluate a scalar integral in the center of momentum/center of mass frame, where $p_i^\alpha \tilde{P}_{T,\alpha} = p_i^0$. In the massless case, $a = \sigma_{ij}(s, \Theta) s \sqrt{s}/4$, in the massive case,

$$\begin{aligned} a_{ij}(s) &= \gamma_{ij} \int \frac{d^3p}{p_i^0} \frac{d^3p'}{p_j^0} s \sigma_{ij}(s, \Theta) \delta(p_i^0 + p_j^0 - \sqrt{s}) \delta^{(3)}(\mathbf{p}_i + \mathbf{p}'_j) p_i^0 \\ &= \gamma_{ij} \int \frac{|\mathbf{r}|^2 d|\mathbf{r}|}{p_i^0 p_j^0} s \sigma_{ij}(s, \Theta) \delta(p_i^0 + p_j^0 - \sqrt{s}) \delta^{(3)}(\mathbf{p}_i + \mathbf{p}'_j) p_i^0 \\ &= \frac{1}{2} \left(\gamma_{ij} \int d\Omega \sigma_{ij}(s, \Theta) \right) \sqrt{(s - s_a^{ij})(s - s_b^{ij})} \sqrt{\frac{1}{4s} (s - s_a^{ij})(s - s_b^{ij}) + m_i^2} \end{aligned} \quad (\text{A4})$$

where we defined

$$|\mathbf{r}| = \frac{1}{2x} \sqrt{(x^2 - (m_i + m_j)^2)(x^2 - (m_i - m_j)^2)}, \quad s_a^{ij} = (m_i + m_j)^2, \quad s_b^{ij} = (m_i - m_j)^2, \quad x = p_i^0 + p_j^0, \quad (\text{A5})$$

and use

$$\frac{dx}{x} = \frac{|\mathbf{r}| d|\mathbf{r}|}{p_i^0 p_j^0}. \quad (\text{A6})$$

The $dK dK'$ -integrals of Eq. (19) are easily done in the massless case, but require numerical integration in the massive case.

Appendix B: Cross-sections for pion-Isotriplett elastic scattering via ρ resonances

As an example for the resonance cross sections, the total cross-section for the reaction

$$\pi^\pm + \pi^\mp \rightarrow \rho^0 \rightarrow \pi^\pm + \pi^\mp \quad (\text{B1})$$

is given by (we use the parametrisation given e.g. in [70, 71])

$$\sigma_{\text{tot}}(\sqrt{s}) = \langle j_{\pi^\mp}, m_{\pi^\mp}, j_{\pi^\pm}, m_{\pi^\pm} || J_{\rho^0}, M_{\rho^0} \rangle \frac{2S_{\rho^0} + 1}{(2S_{\pi^\mp} + 1)(2S_{\pi^\pm} + 1)} \frac{\pi}{p_{\text{CMS}}^2} \frac{\Gamma_{\rho^0 \rightarrow \pi^\pm + \pi^\mp} \Gamma_{\text{tot}}}{(M_{\rho^0} - \sqrt{s})^2 + \frac{\Gamma_{\text{tot}}^2}{4}} \quad (\text{B2})$$

Here, j, J is the isospin of the particle or resonance, S_{particle} its spin and m, M the z-component of it. The Clebsch-Gordon coefficients can be looked up:

$\langle j_{\pi^\mp}, m_{\pi^\mp}, j_{\pi^\pm}, m_{\pi^\pm} J_{\rho^0}, M_{\rho^0} \rangle$	$\mp \sqrt{\frac{1}{2}}$
$\langle j_{\pi^-}, m_{\pi^-}, j_{\pi^0}, m_{\pi^0} J_{\rho^-}, M_{\rho^-} \rangle$	$-\frac{1}{2}$
$\langle j_{\pi^0}, m_{\pi^0}, j_{\pi^-}, m_{\pi^-} J_{\rho^-}, M_{\rho^-} \rangle$	$\frac{1}{2}$
$\langle j_{\pi^+}, m_{\pi^+}, j_{\pi^0}, m_{\pi^0} J_{\rho^+}, M_{\rho^+} \rangle$	$\frac{1}{2}$
$\langle j_{\pi^0}, m_{\pi^0}, j_{\pi^-}, m_{\pi^-} J_{\rho^-}, M_{\rho^-} \rangle$	$-\frac{1}{2}$

The Center-of-Mass momentum is given by

$$p_{\text{CMS}} = \frac{1}{2\sqrt{s}} \sqrt{(s - (m_{\pi^+} + m_{\pi^-})^2) \cdot (s - (m_{\pi^+} - m_{\pi^-})^2)}. \quad (\text{B3})$$

The widths are themselves energy-dependent:

$$\Gamma_{\rho^0 \rightarrow \pi^\pm + \pi^\mp}(\sqrt{s}) = \Gamma_{\rho^0 \rightarrow \pi^\pm + \pi^\mp}^{\text{pole}} \frac{m_\rho}{\sqrt{s}} \left(\frac{p_{\text{CMS}}(\sqrt{s})}{p_{\text{CMS}}(m_\rho)} \right)^{2l+1} \frac{1.2}{1 + 0.2 \left(\frac{p_{\text{CMS}}(\sqrt{s})}{p_{\text{CMS}}(m_\rho)} \right)^{2l}}, \quad (\text{B4})$$

with an angular momentum l of the decay. We are considering only one decay channel for each process, so $\Gamma_{\text{tot}} = \Gamma_{\text{decay channel}}$.

-
- [1] I. Arsene *et al.* (BRAHMS), Nucl. Phys. **A757**, 1 (2005), arXiv:nucl-ex/0410020.
[2] K. Adcox *et al.* (PHENIX), Nucl. Phys. **A757**, 184 (2005), arXiv:nucl-ex/0410003.
[3] B. B. Back *et al.*, Nucl. Phys. **A757**, 28 (2005), arXiv:nucl-ex/0410022.
[4] J. Adams *et al.* (STAR), Nucl. Phys. **A757**, 102 (2005), arXiv:nucl-ex/0501009.
[5] P. F. Kolb, J. Sollfrank, and U. W. Heinz, Phys. Rev. **C62**, 054909 (2000), arXiv:hep-ph/0006129.
[6] C. Gale, S. Jeon, and B. Schenke, International Journal of Modern Physics A **28**, 1340011 (2013).
[7] B. Schenke, Journal of Physics G, **1** (2011), arXiv:1106.6012v1.
[8] C. Shen and U. Heinz, Phys. Rev. C **85**, 054902 (2012).
[9] P. F. Kolb and U. W. Heinz, (2003), arXiv:nucl-th/0305084.
[10] D. Teaney, J. Lauret, and E. V. Shuryak, Phys. Rev. Lett. **86**, 4783 (2001).
[11] L. Del Zanna, V. Chandra, G. Inghirami, V. Rolando, A. Beraudo, A. De Pace, G. Pagliara, A. Drago, and F. Becattini, Eur. Phys. J. **C73**, 2524 (2013), arXiv:1305.7052.
[12] I. Karpenko, P. Huovinen, and M. Bleicher, Comput. Phys. Commun. **185**, 3016 (2014), arXiv:1312.4160.
[13] H. Holopainen, H. Niemi, and K. J. Eskola, Phys. Rev. **C83**, 034901 (2011), arXiv:1007.0368.
[14] Z. Xu and C. Greiner, Physical Review C **71**, 064901 (2005), arXiv:0406278v2.
[15] I. Bouras, E. Molnár, H. Niemi, Z. Xu, A. El, O. Fochler, C. Greiner, and D. H. Rischke, Physical Review C **82**, 024910 (2010).
[16] I. Bouras, A. El, O. Fochler, H. Niemi, Z. Xu, and C. Greiner, Physics Letters B **710**, 641 (2012), arXiv:1201.5005.
[17] I. Bouras, E. Molnár, H. Niemi, Z. Xu, A. El, O. Fochler, C. Greiner, and D. H. Rischke, Physical Review Letters **103**, 032301 (2009).
[18] O. Fochler, Z. Xu, and C. Greiner, Physical Review C **82**, 024907 (2010), arXiv:1003.4380.
[19] O. Fochler, Z. Xu, and C. Greiner, Nuclear Physics A **855**, 420 (2011), arXiv:1012.1811.
[20] J. Uphoff, O. Fochler, Z. Xu, and C. Greiner, Physical Review C **84**, 024908 (2011), arXiv:1104.2295.
[21] C. Wesp, A. El, F. Reining, Z. Xu, I. Bouras, and C. Greiner, Physical Review C **84**, 054911 (2011), arXiv:1106.4306.
[22] F. Reining, I. Bouras, A. El, C. Wesp, Z. Xu, and C. Greiner, Physical Review E **85**, 026302 (2012), arXiv:1106.4210.
[23] J. Uphoff, O. Fochler, Z. Xu, and C. Greiner, Physics Letters B **717**, 430 (2012), arXiv:1205.4945.
[24] O. Fochler, J. Uphoff, Z. Xu, and C. Greiner, Physical Review D **88**, 014018 (2013), arXiv:1302.5250.
[25] M. Greif, F. Reining, I. Bouras, G. S. Denicol, Z. Xu, and C. Greiner, Physical Review E **87**, 033019 (2013), arXiv:1301.1190.
[26] F. Senzel, O. Fochler, J. Uphoff, Z. Xu, and C. Greiner, J. Phys. **G42**, 115104 (2015), arXiv:1309.1657.
[27] J. Uphoff, O. Fochler, Z. Xu, and C. Greiner, Nuclear Physics A **910-911**, 401 (2013), arXiv:1208.1970.
[28] M. Gyulassy and L. McLerran, Nuclear Physics A **750**, 30 (2005).
[29] B. Schenke, S. Jeon, and C. Gale, Physical Review Letters **106**, 042301 (2011).
[30] S. Plumari, A. Puglisi, F. Scardina, and V. Greco, Physical Review C **86**, 054902 (2012).
[31] M. Greif, I. Bouras, C. Greiner, and Z. Xu, Phys. Rev. D **90**, 094014 (2014), arXiv:1408.7049.
[32] A. Puglisi, S. Plumari, and V. Greco, arXiv:1407.2559, **5** (2014), arXiv:1407.2559.
[33] A. Puglisi, S. Plumari, and V. Greco, Phys. Rev. D **90**, 114009 (2014), arXiv:1408.7043.
[34] G. S. Denicol, H. Niemi, E. Molnar, and D. H. Rischke, Physical Review D **85**, 114047 (2012), arXiv:1202.4551.
[35] G. S. Denicol, E. Molnár, H. Niemi, and D. H. Rischke, The European Physical Journal A **48**, 170 (2012), arXiv:1206.1554.
[36] G. S. Denicol, T. Koide, and D. H. Rischke, Physical Review Letters **105**, 162501 (2010), arXiv:1004.5013.
[37] G. Baym and H. Heiselberg, Physical Review D **56**, 11 (1997), arXiv:9704214.
[38] K. Tuchin, **67** (2013), arXiv:1301.0099.
[39] D. Fernández-Fraile and A. Gomez Nicola, Physical Review D **73**, 045025 (2006).
[40] G. D. Moore and J. M. Robert, hep-ph/0607172 (2006), arXiv:0607172v1.
[41] H.-T. Ding, O. Kaczmarek, and F. Meyer, (2016), arXiv:1604.06712 [hep-lat].
[42] J. Ghiglieri, O. Kaczmarek, M. Laine, and F. Meyer, (2016), arXiv:1604.07544 [hep-lat].

- [43] S. Endres, H. van Hees, J. Weil, and M. Bleicher, Phys. Rev. **C92**, 014911 (2015), arXiv:1505.06131 [nucl-th].
- [44] W. Cassing, O. Linnyk, T. Steinert, and V. Ozvenchuk, Physical Review Letters **110**, 182301 (2013), arXiv:1302.0906.
- [45] T. Steinert and W. Cassing, Physical Review C **89**, 035203 (2014), arXiv:1312.3189.
- [46] S. I. Finazzo and J. Noronha, Physical Review D **89**, 106008 (2014), arXiv:1311.6675.
- [47] G. Aarts, C. Allton, A. Amato, P. Giudice, S. Hands, and J.-I. Skullerud, JHEP **02**, 186 (2015), arXiv:1412.6411.
- [48] G. Aarts, C. Allton, J. Foley, S. Hands, and S. Kim, Physical Review Letters **99**, 022002 (2007).
- [49] B. B. Brandt, A. Francis, H. B. Meyer, and H. Wittig, Journal of High Energy Physics **2013**, 100 (2013).
- [50] A. Amato, G. Aarts, C. Allton, P. Giudice, S. Hands, and J.-I. Skullerud, Physical Review Letters **111**, 172001 (2013), arXiv:1307.6763.
- [51] S. Gupta, Physics Letters B **597**, 57 (2004).
- [52] P. V. Buividovich, M. N. Chernodub, D. E. Kharzeev, T. Kalaydzhyan, E. V. Luschevskaya, and M. I. Polikarpov, Physical Review Letters **105**, 132001 (2010).
- [53] Y. Burnier and M. Laine, The European Physical Journal C **72**, 1 (2012).
- [54] H.-T. Ding, A. Francis, O. Kaczmarek, F. Karsch, E. Laermann, and W. Soeldner, Physical Review D **83**, 034504 (2011).
- [55] O. Kaczmarek and M. Müller, PoS LATTICE2013, 175 (2014), arXiv:1312.5609.
- [56] S.-X. Qin, Phys. Lett. **B742**, 358 (2015), arXiv:1307.4587.
- [57] P. Arnold, G. D. Moore, and L. G. Yaffe, Journal of High Energy Physics **2000**, 001 (2000), arXiv:hep-ph/0010177.
- [58] J.-W. Chen, Y.-F. Liu, S. Pu, Y.-K. Song, and Q. Wang, Phys. Rev. D **88**, 085039 (2013).
- [59] R. Marty, E. Bratkovskaya, W. Cassing, J. Aichelin, and H. Berrehrah, Phys. Rev. **C88**, 045204 (2013), arXiv:1305.7180.
- [60] H. Berrehrah, W. Cassing, E. Bratkovskaya, and T. Steinert, (2015), arXiv:1512.06909.
- [61] G. S. Denicol, J. Noronha, H. Niemi, and D. H. Rischke, Phys. Rev. **D83**, 074019 (2011), arXiv:1102.4780.
- [62] G. S. Denicol, J. Noronha, H. Niemi, and D. H. Rischke, J. Phys. **G38**, 124177 (2011), arXiv:1108.6230.
- [63] G. S. Denicol, C. Gale, S. Jeon, and J. Noronha, Phys. Rev. C **88**, 064901 (2013), arXiv:1308.1923.
- [64] S. R. Groot, W. van Leeuwen, and van Weert Ch.G., *Relativistic Kinetic Theory-Principles and Applications* (North-Holland, Amsterdam, 1980).
- [65] D. Molnar and Z. Wolff, (2014), arXiv:1404.7850.
- [66] A. Bazavov *et al.*, Phys. Rev. D **85**, 054503 (2012), arXiv:1111.1710.
- [67] S. C. Huot, P. Kovtun, G. D. Moore, A. Starinets, and L. G. Yaffe, Journal of High Energy Physics **2006**, 015 (2006), arXiv:0607237 [hep-th].
- [68] R. Rougemont, J. Noronha, and J. Noronha-Hostler, Phys. Rev. Lett. **115**, 202301 (2015), arXiv:1507.06972.
- [69] W. Cassing, V. Metag, U. Mosel, and K. Niita, Phys. Rept. **188**, 363 (1990).
- [70] S. A. Bass *et al.*, Prog. Part. Nucl. Phys. **41**, 255 (1998), [Prog. Part. Nucl. Phys.41,225(1998)], arXiv:nucl-th/9803035.
- [71] M. Bleicher, E. Zabrodin, C. Spieles, S. A. Bass, C. Ernst, S. Soff, L. Bravina, M. Belkacem, H. Weber, H. Stcker, and W. Greiner, Journal of Physics G: Nuclear and Particle Physics **25**, 1859 (1999).
- [72] O. Buss, T. Gaitanos, K. Gallmeister, H. van Hees, M. Kaskulov, O. Lalakulich, A. B. Larionov, T. Leitner, J. Weil, and U. Mosel, Phys. Rept. **512**, 1 (2012), arXiv:1106.1344.
- [73] K. A. Olive *et al.* (Particle Data Group), Chin. Phys. **C38**, 090001 (2014).